A Dynamic and Anisotropic Vector Hysteresis Model Based on Isotropic Vector Play Model for Non-Oriented Silicon Steel Sheet

Tetsuji Matsuo and Masaki Miyamoto
Kyoto University
Kyotodaigaku-katsura, Nishikyo-ku, Kyoto, 615-8510, Japan
tmatsuo@kuee.kyoto-u.ac.jp

Abstract — A phenomenological vector hysteresis model is developed to represent dynamic and anisotropic vector hysteretic properties of non-oriented silicon steel sheets. The anisotropic vector hysteresis is represented by the multiplication of an anisotropy matrix and an isotropic vector play model. An eddy-current field vector given by classical eddy-current theory and an anomaly factor is added to the vector hysteresis model. The anomaly factor is determined to model the decrease in anomalous eddy-current loss for large rotational magnetic flux. The alternating and rotational properties simulated by the proposed model reconstruct the measured magnetic properties of non-oriented silicon steels.

I. Introduction

It is not easy for the conventional finite element magnetic field analysis to handle the anomalous (or excess) eddy-current (EC) loss [1] yielded by a laminated iron core because the magnetic-domain size of silicon steel is much smaller than the core size. To describe the influence of EC field, several hysteresis models have dynamic terms that can represent the anomalous EC loss accurately in the presence of alternating magnetic flux [2-4]. However, the extension of the dynamic scalar hysteresis model to the vector model [5, 6] is not straightforward because large rotational magnetic flux does not induce the domain-wall motion that causes the anomalous EC loss.

Based on the measured eddy-current loss for alternating and rotational fluxes, this paper proposes a simple method to represent the anomaly factor. A phenomenological vector hysteresis model is developed for an accurate and efficient representation of the dynamic and weakly anisotropic vector hysteretic properties of non-oriented (NO) silicon steel sheets.

II. Static Vector Play Models

A. Isotropic Vector Play Mode

The play model is an efficient and precise hysteresis model, which has several vector versions [7-9]. A static and isotropic vector play model [9] provides an output of magnetic field $\boldsymbol{H}$ from an input of magnetic flux density $\boldsymbol{B}$:

$$\boldsymbol{H} = \boldsymbol{P}(\boldsymbol{B}) = \int_0^{B_S} \boldsymbol{f}(\zeta, \boldsymbol{p}_\zeta(\boldsymbol{B}))\mathrm{d}\zeta \quad (1)$$

$$\boldsymbol{f}(\zeta, \boldsymbol{p}) = f(\zeta, |\boldsymbol{p}|)\, \boldsymbol{p} / |\boldsymbol{p}| \quad (2)$$

where $f(\zeta, p)$ is a shape function, B_S is the saturation magnetic flux density, and $\boldsymbol{p}_\zeta$ is a vector play hysteron of radius ζ. Hysteron $\boldsymbol{p}_\zeta$ is given by:

$$\boldsymbol{p}_\zeta(\boldsymbol{B}) = \boldsymbol{B} - \zeta(\boldsymbol{B} - \boldsymbol{p}_\zeta^{\,0}) / \max(\zeta, |\boldsymbol{B} - \boldsymbol{p}_\zeta^{\,0}|) \quad (3)$$

where $\boldsymbol{p}_\zeta^0$ is the vector $\boldsymbol{p}_\zeta$ at the previous time-point.

The isotropic vector play model is identified from the alternating property with the input of $\boldsymbol{B}_{\mathrm{alt}} = B_{\mathrm{a}}\cos\omega t\,(\cos\phi_B, \sin\phi_B)$ where B_{a} is the amplitude and ϕ_B is the azimuth angle. The measured alternating property is represented by $\boldsymbol{H}_{\mathrm{alt}}(B, \phi_B)$ that is given by $\boldsymbol{H}_{\mathrm{alt}}(B_{\mathrm{a}}\cos\omega t, \phi_B) = \boldsymbol{H}(\boldsymbol{B}_{\mathrm{alt}})$. The averaged alternating property is given by

$$H_{\mathrm{ave}}(B) = 1/\pi \int_0^{\pi} \boldsymbol{H}_{\mathrm{alt}}(B, \phi)\cdot\boldsymbol{e}_\phi \mathrm{d}\phi \quad (4)$$

where $\boldsymbol{e}_\phi$ is the unit vector along the ϕ-direction. Shape function f is determined from measured $H_{\mathrm{ave}}(B)$ via the identification method for a scalar play model.

To adjust the simulated rotational hysteresis loss to the measured values, the play model (1) is modified [10]:

$$\boldsymbol{P}^*(\boldsymbol{B}) = (\boldsymbol{P}(\boldsymbol{B})\cdot\boldsymbol{e}_\parallel)\boldsymbol{e}_\parallel + \boldsymbol{r}(|\boldsymbol{B}|)(\boldsymbol{P}(\boldsymbol{B})\cdot\boldsymbol{e}_\perp)\boldsymbol{e}_\perp \quad (5)$$

where $\boldsymbol{e}_\parallel$ and $\boldsymbol{e}_\perp$ denote the unit vectors parallel and perpendicular to $\boldsymbol{B}$, respectively, and $r(B_{\mathrm{a}})$ is the ratio of the measured hysteresis loss to the simulated loss given by $\boldsymbol{P}$ for the rotational input of $\boldsymbol{B}_{\mathrm{rot}} = (B_{\mathrm{a}}\cos\omega t, B_{\mathrm{a}}\sin\omega t)$.

B. Anisotropic Vector Play Model

A simple 2D anisotropic version of the vector play model [10] is:

$$\boldsymbol{P}_{\mathrm{an}}(\boldsymbol{B}) = \boldsymbol{W}_B(\boldsymbol{B})\, \boldsymbol{P}^*(\boldsymbol{B}) \quad (6)$$

where $\boldsymbol{W}_B(\boldsymbol{B})$ is an anisotropy matrix whose components are single-valued functions of $\boldsymbol{B}$. For example, $\boldsymbol{W}_B(\boldsymbol{B})$ is determined to approximately reconstruct the anisotropic alternating property from the averaged alternating property:

$$\boldsymbol{W}_B(\boldsymbol{B}) = \mathrm{diag}\left(\frac{H_{\mathrm{altx}}(B_{\mathrm{a}}, \phi_B)}{H_{\mathrm{ave}}(B_{\mathrm{a}})\cos\phi_B}, \frac{H_{\mathrm{alty}}(B_{\mathrm{a}}, \phi_B)}{H_{\mathrm{ave}}(B_{\mathrm{a}})\sin\phi_B}\right) \quad (7)$$

where $(H_{\mathrm{altx}}(B, \phi_B), H_{\mathrm{alty}}(B, \phi_B)) = \boldsymbol{H}_{\mathrm{alt}}(B, \phi_B)$. The maximum point of alternating input of $\boldsymbol{B}_{\mathrm{alt}} = (B_{\mathrm{a}}\cos\phi_B, B_{\mathrm{a}}\sin\phi_B)$ and the corresponding output H_{ave} and measured $\boldsymbol{H}_{\mathrm{alt}}$ are used to determine $\boldsymbol{W}_B$.

III. A Dynamic Vector Play Model

A simple vectorization of a dynamic scalar play model [2] is given by:

$$\boldsymbol{H} = \boldsymbol{P}_{\mathrm{dy}}(\boldsymbol{B}, \mathrm{d}\boldsymbol{B}/\mathrm{d}t) = \boldsymbol{P}_{\mathrm{an}}(\boldsymbol{B}) + k\,(\sigma d^2/12)\,(\mathrm{d}\boldsymbol{B}/\mathrm{d}t)^\gamma \quad (8)$$

where $(\mathrm{d}\boldsymbol{B}/\mathrm{d}t)^\gamma = ((\mathrm{d}B_x/\mathrm{d}t)^\gamma, (\mathrm{d}B_y/\mathrm{d}t)^\gamma)$ and X^γ means $\mathrm{sign}(X)|X|^\gamma$; k is the anomaly factor, σ is the electrical conductivity, d is the sheet thickness, and γ represents the frequency dependence of eddy-current field. This paper assumes that $\gamma = 1$. When $\gamma = 1$, the vector model (8) yields the EC loss of $L_{\mathrm{ed}} = k\,L_{\mathrm{cl}}$ where L_{cl} is the classical EC loss [1] per cycle; L_{cl} is given by $\pi\omega\sigma d^2 B_{\mathrm{a}}^2/12$ for the alternating input $\boldsymbol{B}_{\rm alt}$ with the amplitude $B_{\rm a}$ whereas it is $\pi\omega\sigma d^2 B_{\rm a}^2/6$ for the rotational input $\boldsymbol{B}_{\rm rot}$.

The anomaly factor $k = L_{\rm ed}/L_{\rm cl}$ was measured for two NO steel sheets, JIS: 35A350 and 35A230. Figs. 1 and 2 show the anomaly factors of the two sheets, respectively, under conditions of alternating and rotational flux where the averaged values with respect to the azimuth angle ϕ_B and the amplitude $B_{\rm a}$ are shown for alternating flux condition. The anomaly factor is roughly constant for the alternating flux, but it decreases for the large rotational flux where the magnetization rotation becomes dominant. Thereby, the anomalous EC loss caused by the domain-wall motion decreases for the large rotational inputs.

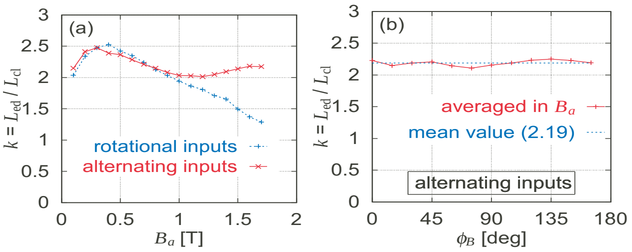

Fig. 1. Measured anomaly factor of 35A350: (a) dependence on amplitude and (b) dependence on azimuth angle

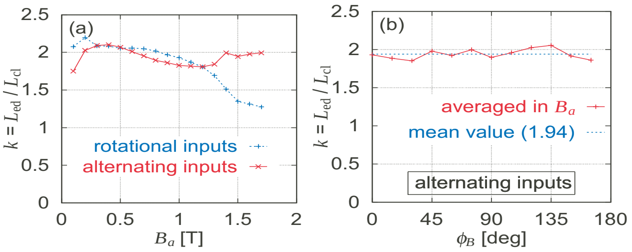

Fig. 2. Measured anomaly factor of 35A230: (a) dependence on amplitude and (b) dependence on azimuth angle

Focusing on the decrease in k under conditions of rotational flux, this paper ignores the dependence of k on B under conditions of alternating flux and gives k as

$$k(|\boldsymbol{B}|,\theta)=\begin{cases} k_0 & (|\boldsymbol{B}|\le B_{\rm R}) \\ k_0+(1-k_0)\dfrac{1-\cos 2\theta}{2}\dfrac{B^*-B_{\rm R}}{B_{\rm S}-B_{\rm R}} & (B_{\rm R}<|\boldsymbol{B}|) \end{cases} \quad (9)$$

where $B^* = \min(|\boldsymbol{B}|, B_{\rm S})$ and k_0 and $B_{\rm R}$ are constants; θ is the angle between $\boldsymbol{B}$ and $\mathrm{d}\boldsymbol{B}/\mathrm{d}t$, which is $\pm\pi/2$ for rotational flux.

Fig. 3 shows the simulated and measured iron losses of 35A350 for the alternating and rotational inputs with the frequency f = 10, 50, 100, 200 Hz. The constants for k are given as k_0 = 2.19, $B_{\rm R}$ = 0.8 T, and $B_{\rm S}$ = 2 T; $B_{\rm S}$ is treated as a simulation parameter and does not correspond to the real value of the saturation magnetization.

The simulated loss agrees with the measured loss when $f \le 100$ Hz, but it is larger than the measured loss for f = 200 Hz. This implies that the EC loss per cycle is not proportional to f. The discrepancy is probably caused by the skin effect or the domain-wall bowing [1, 3]. The simulated iron loss at 200 Hz is adjusted to the measured loss by setting γ = 0.94, which will be addressed in the extended paper.

Fig. 4(a) portrays the simulated loci of $\boldsymbol{H}$ of 35A300 for the counterclockwise (CCW) rotational inputs of $\boldsymbol{B}$ where $B_{\rm a}$ = 1.4, 1.5, 1.6 T and f = 10, 100 Hz, which agree with the measured loci.

Fig. 4(b) shows the simulated loci of $\boldsymbol{H}$ under the condition of elliptically rotational flux where the azimuth angle of the major axis is $\pi/4$ and the axial ratio is 0.5. The simulated loci approximately reconstruct the measured ones.

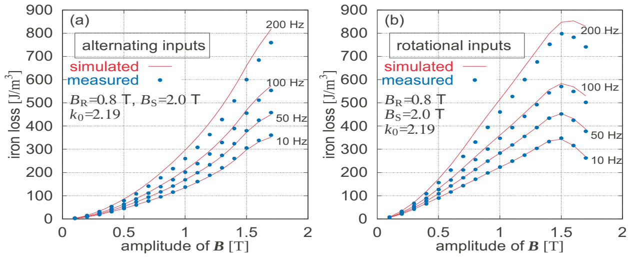

Fig. 3. Iron losses per cycle of 35A350: (a) alternating flux and (b) rotational flux

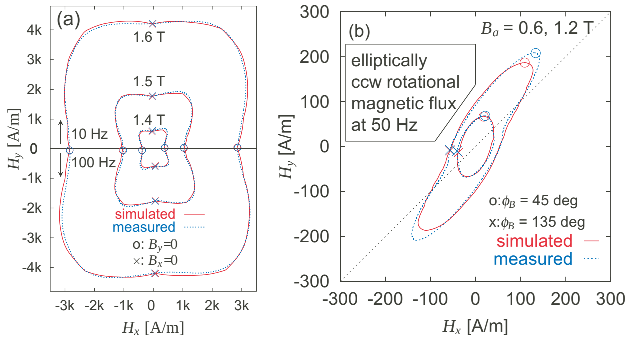

Fig. 4. Loci of $\boldsymbol{H}$ for rotational and elliptically rotational fluxes; (a) rotational flux with $B_{\rm a}$ = 1.4, 1.5, 1.6 T where B_x = 0 at "o" and B_y = 0 at "x", (b) elliptically rotational flux where $\phi_B = \pi/4$ at "o" and $3\pi/4$ at "x"

IV. References

[1] G. Bertotti, *Hysteresis in Magnetism*, Academic Press: , 1998.

[2] T. Matsuo and M. Shimasaki, "Simple modeling of the AC hysteretic property of a grain-oriented silicon steel sheet," *IEEE Trans. Magn.*, vol. 42, no. 4, pp. 919-922, 2006.

[3] S. E. Zirka, Y. I. Moroz, P. Marketos, A. J. Moses, D. C. Jiles and T. Matsuo, "Generalization of the classical method for calculating dynamic hysteresis loops in grain oriented electrical steels," *IEEE Trans. Magn.*, vol. 44, no. 9, pp. 2113-2126, 2008.

[4] E. Dlala, "A simplified iron loss model for laminated magnetic cores," *IEEE Trans. Magn.*,vol. 44, no. 11, pp. 3169-3172, 2008.

[5] E. Dlala, A. Belahcen, and A. Arkkio, "Magnetodynamic vector hysteresis model of ferromagnetic steel laminations," *Physica B*, vol. 403, issue 2-3, pp. 428-432, 2008.

[6] M. Enokizono, T. Todaka, S. Urata, "Dynamic vector magneto-hysteretic E&S model considering eddy current effect," *COMPEL*, vol. 28, no. 1, pp. 85-97, 2009.

[7] A. Bergqvist, "Magnetic vector hysteresis model with dry friction-like pinning," *Physica B*, vol. 233, pp. 342-347, 1997.

[8] C. Serpico, M. d'Aquino, C. Visone and D. Davino, "A new class of Preisach-type isotropic vector model of hysteresis," *Physica B*, vol. 343, pp. 117-120, 2004.

[9] T. Matsuo and M. Shimasaki, "Two types of isotropic vector play models and their rotational hysteresis losses," *IEEE Trans. Magn.*, vol. 44, no. 6, pp. 898-901, 2008.

[10] T. Matsuo, "Anisotropic vector hysteresis model using an isotropic vector play model," *IEEE Trans. Magn.*, vol. 46, no. 8, pp. 3041-3044, 2010.